Near-Field Thermal Transistor

Philippe Ben-Abdallah*
Laboratoire Charles Fabry, UMR 8501, Institut d'Optique, CNRS, Université Paris-Sud 11, 2, Avenue Augustin Fresnel, 91127 Palaiseau Cedex, France

Svend-Age Biehs†
Institut für Physik, Carl von Ossietzky Universität, D-26111 Oldenburg, Germany
(Received 16 September 2013; published 31 January 2014)

Using a block of three separated solid elements, a thermal source and drain together with a gate made of an insulator-metal transition material exchanging near-field thermal radiation, we introduce a nanoscale analog of a field-effect transistor that is able to control the flow of heat exchanged by evanescent thermal photons between two bodies. By changing the gate temperature around its critical value, the heat flux exchanged between the hot body (source) and the cold body (drain) can be reversibly switched, amplified, and modulated by a tiny action on the gate. Such a device could find important applications in the domain of nanoscale thermal management and it opens up new perspectives concerning the development of contactless thermal circuits intended for information processing using the photon current rather than the electric current.

DOI: 10.1103/PhysRevLett.112.044301 PACS numbers: 44.40.+a, 05.60.-k, 78.67.-n

The electronic solid-state transistor [Fig. 1(a)] introduced by Bardeen and Brattain in 1948 [1] is undoubtedly the cornerstone of almost all modern systems of information treatment. The classical field-effect transistor (FET), which is composed of three basic elements, the drain, the source, and the gate, is basically used to control the flux of electrons (the current) exchanged in the channel between the drain and the source by changing the voltage applied on the gate. The physical diameter of this channel is fixed, but its effective electrical diameter can be varied by the application of a voltage on the gate. A small change in this voltage can cause a large variation in the current from the source to the drain. In 2006, Li *et al.* [2] proposed a thermal counterpart of FET by replacing both the electric potentials and the electric currents by thermostats at a fixed temperature and heat fluxes carried by phonons through solid segments. Later, several prototypes of phononic thermal logic gates [3] as well as thermal memories (see [4] and references therein) were developed in order to process information by phonon heat flux rather than by electric currents. However, this technology suffers from some fundamental weaknesses which intrinsically limit its performance. One of the main limitations probably comes from the speed of acoustic phonons (heat carriers), which is 4 or 5 orders of magnitude smaller than the speed of photons. Another intrinsic limitation of phononic devices is related to the inevitable presence of local Kapitza resistances. Those resistances which come from the mismatch of vibrational modes at the interface of different elements can reduce the heat flux dramatically. Finally, the strong nonlinear phonon-phonon interaction mechanism makes the phononic devices difficult to deal with in the presence of a strong thermal gradient. On the contrary, the physics of transport mediated by photon tunneling remains unchanged close and far from thermal equilibrium. This explains, in part, why so many efforts have been deployed, during the past decades, to attempt to develop full optical or at least optoelectronic architectures for processing and managing information. In particular, important developments have been carried out during the past decade with plasmonics systems [5,6] to greatly increase the speed of information processing while reducing the dimension of devices at the nanoscale at the same time. However, despite these major steps forward, an optical transistor is still missing.

We introduce here a thermal transistor [Fig. 1(b)] based on the heat transport by evanescent photons rather than by acoustic waves or electrons. This near-field thermal transistor (NFTT) basically consists of a gate made of an insulator-metal transition (IMT) material which is able to qualitatively and quantitatively change its optical properties through a small change of its temperature around a critical temperature T_c. Vanadium dioxide (VO_2) is one of such materials (the choice of IMT depends on the operating range of the transistor: around $T = 500$ K, $LaCoO_3$ could replace VO_2, for instance) that undergoes a first-order transition (Mott transition [7]) from a high-temperature metallic phase to a low-temperature insulating phase [8] close to room temperature ($T_c = 340$ K). Different works have already shown [9–11] that the heat flux exchanged at close separation distances (i.e., in the near-field regime) between an IMT material and another medium can be modulated by several orders of magnitude across the phase transition of IMT materials. Further radiative thermal diodes have been recently conceived allowing for

 © 2014 American Physical Society

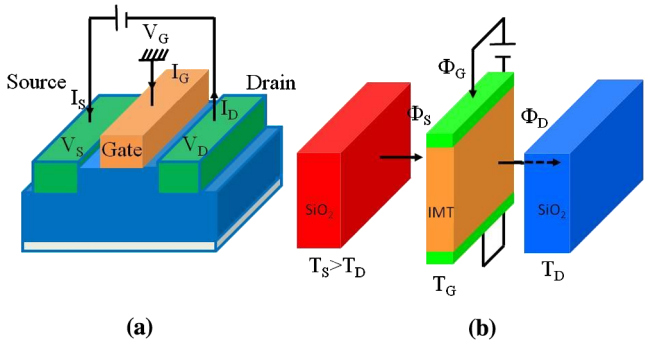

FIG. 1 (color online). Electric and radiative thermal transistor. Classical field-effect transistor (a). A three-terminal device known as source, gate, and drain, which corresponds to the emitter, base, and collector of electrons. The gate is used to actively control, by applying a potential on it, the apparent conductivity of the channel between the source and the drain. Radiative thermal transistor (b). A layer of IMT material (the gate) is placed at subwavelength distances from two thermal reservoirs (the source and the drain). The temperatures T_S and T_D are fixed so that $T_S > T_D$. The temperature T_G of the gate can be modulated from the external environment around its steady-state temperature T_G^{eq} (which corresponds to the situation where the net flux Φ_G received by the gate vanishes) so that the flux Φ_D received by the drain and lost by the source Φ_S can be tuned. When T_G^{eq} is a little bit smaller than the critical temperature T_c of IMT material, a small amount of heat applied on the gate induces a strong switching of heat fluxes Φ_D and Φ_S owing to its metal-insulator phase transition.

rectification [12,13] of heat flux using materials with thermally dependant refractive indices [14–16] and IMT materials [17]. But so far controlling the heat flow with contactless systems to get the same functionalities as a classical FET has remained a challenging problem. Here we show that IMT materials are very promising candidates for designing efficient gates to control (switch, modulate, or amplify) the heat flux exchanged between two media.

To start, let us consider the system as illustrated in Fig. 1(b), where two media, which we call by analogy to a FET the source and the drain labeled by the indices S and D, are maintained at temperatures T_S and T_D with $T_S > T_D$ by some thermostats. A thin layer of IMT material labeled by G having a thickness δ is placed between both media at a distance d from the source and the drain. Without external excitation, the system reaches its steady state for which the net flux Φ_G received by the intermediate medium, the gate, is zero. In this case, its temperature T_G is set by the temperature of the surrounding media, i.e., the drain and the source. When a certain amount of heat is added to or removed from the gate [for example, by applying a voltage difference through a couple of electrodes as illustrated in Fig. 1(b) or extracted from it using Peltier elements], its temperature can be either increased or reduced around its equilibrium temperature T_G^{eq}. Hence, the heat flux Φ_D received by the drain and the flux Φ_S lost by the source can be tailored accordingly. These fluxes correspond to the flux of the Poynting vector across any plane separating the gate and the drain (or the source and the gate). In a three-body system, the flux received by photon tunneling by the drain reads [18]

$$\Phi_D = \int_0^\infty \frac{d\omega}{2\pi} \varphi_D(\omega, d), \tag{1}$$

where the monochromatic heat flux is given by

$$\varphi_D = \hbar\omega \sum_{j=\{s,p\}} \int \frac{d^2\boldsymbol{\kappa}}{(2\pi)^2} [n_{SG}(\omega)\mathcal{T}_j^{S/G}(\omega, \boldsymbol{\kappa}; d) + n_{GD}(\omega)\mathcal{T}_j^{G/D}(\omega, \boldsymbol{\kappa}; d)]. \tag{2}$$

Here ,$\mathcal{T}_j^{S/G}$ and $\mathcal{T}_j^{G/D}$ denote the efficiencies of the coupling of each mode $(\omega, \boldsymbol{\kappa})$ between the source and the gate and between the gate and the drain for both polarization states $j = s,\ p$; $\boldsymbol{\kappa} = (k_x, k_y)^t$ is the wave vector parallel to the surfaces of the multilayer system. In the above relation, n_{ij} denotes the difference of Bose-distribution functions n_i and n_j [with $n_{i/j} = 1/[\exp(\hbar\omega/k_B T_{i/j}) - 1]$] at the frequency ω; k_B is Boltzmann's constant and $2\pi\hbar$ is Planck's constant. According to the N-body near-field heat transfer theory presented in Ref. [18], the transmission coefficients $\mathcal{T}_j^{S/G}$ and $\mathcal{T}_j^{G/D}$ of the energy carried by each mode written in terms of optical reflection coefficients $\rho_{E,j}$ $(E = S, D, G)$ and transmission coefficients $\tau_{E,j}$ of each basic element of the system and in terms of reflection coefficients $\rho_{EF,j}$ of couples of elementary elements are [18]

$$\mathcal{T}_j^{S/G}(\omega, \boldsymbol{\kappa}, d) = \frac{4|\tau_{G,j}|^2 \mathrm{Im}(\rho_{S,j})\,\mathrm{Im}(\rho_{D,j}) e^{-4\gamma d}}{|1 - \rho_{SG,j}\rho_{D,j} e^{-2\gamma d}|^2 |1 - \rho_{S,j}\rho_{G,j} e^{-2\gamma d}|^2},$$
$$\mathcal{T}_j^{G/D}(\omega, \boldsymbol{\kappa}, d) = \frac{4\,\mathrm{Im}(\rho_{SG,j})\,\mathrm{Im}(\rho_{D,j}) e^{-2\gamma d}}{|1 - \rho_{SG,j}\rho_{D,j} e^{-2\gamma d}|^2}, \tag{3}$$

introducing the imaginary part of the wave vector normal to the surfaces in the multilayer structure $\gamma = \mathrm{Im}(k_z) = \sqrt{\kappa^2 - \omega^2/c^2}$; c is the velocity of light in vacuum. Similarly, the heat flux lost by the source reads

$$\phi_S = \hbar\omega \sum_{j=\{s,p\}} \int \frac{d^2\boldsymbol{\kappa}}{(2\pi)^2} [n_{DG}(\omega)\mathcal{T}_j^{D/G}(\omega, \boldsymbol{\kappa}; d) + n_{GS}(\omega)\mathcal{T}_j^{G/S}(\omega, \boldsymbol{\kappa}; d)], \tag{4}$$

where the transmission coefficients are analog to those defined in Eq. (3) and can be obtained making the substitution $S \leftrightarrow D$.

At steady state, the net heat flux received or emitted by the gate vanishes. It is just given by the heat flux from the source to the gate minus the heat flux from the gate to the drain, i.e., in steady state $\Phi_S = \Phi_D$ or

$$\Phi_G = \Phi_S - \Phi_D = 0. \quad (5)$$

This relation allows us to identify the gate equilibrium temperature T_G^{eq} (which is not necessarily unique) for given temperatures T_S and T_D. Note that out of the steady state the heat flux received or emitted by the gate is $\Phi_G = \Phi_S - \Phi_D \neq 0$. If $\Phi_G < 0$ ($\Phi_G > 0$), an external flux is added to (removed from) the gate by heating (cooling).

To illustrate the operating modes of NFTT, we now consider a system composed of a source and a drain both made of silica (each coupled to a thermostat to maintain their local temperatures constant in time) and a gate made of vanadium dioxide VO_2. When the gate temperature T_G is smaller than its critical temperature T_c, then the gate is in its monoclinic phase and it behaves as a uniaxial crystal. On the other hand, when $T_G = T_c$, the gate transits toward its amorphous metallic phase and remains in this state for greater temperatures. Here we consider the case where the optical axis of VO_2 film is orthogonal to its interfaces. The p-polarized transmission coefficients of the energy carried by the modes (ω, $\boldsymbol{\kappa}$) through such a system are plotted in Fig. 2. When the gate is in its crystalline state, $\mathcal{T}_p^{S/G}$ [see Fig. 2(a)] and $\mathcal{T}_p^{G/D}$ [see Fig. 2(b)] show an efficient coupling of modes between the different blocks of the system around the resonance frequencies $\omega_{\mathrm{SPP1}} \sim 1 \times 10^{14}$ rad/s and $\omega_{\mathrm{SPP2}} \sim 2 \times 10^{14}$ rad/s of surface waves (surfaces phonon-polaritons) supported by both the source and the drain. Note that $\mathcal{T}_p^{S/G}$ represents the exchange between the source and the drain mediated by the presence of the gate while $\mathcal{T}_p^{G/D}$ corresponds to the exchange between the couple source-gate, treated as a unique body, and the drain. Below T_c all parts of the system support surface waves in the same frequency range close to the thermal peak frequency $\omega_{\mathrm{Wien}} \sim 1.3 \times 10^{14}$ rad/s. The anticrossing curves that appear in Figs. 2(a) and 2(b) result from the strong coupling of silica surface phonon polaritons (SPPs) and the surface waves (symmetric and antisymmetric ones) supported by the thin VO_2 layer. Beyond T_c the gate becomes amorphous (metallic) and it does not support surface waves anymore. In this case, $\mathcal{T}_p^{S/G}$ [see Fig. 2(c)] vanishes owing to the field screening by the gate. Moreover, as is clearly shown in Fig. 2(d), the coupling of modes between the couple source gate and the drain at the frequency of the surface waves is less efficient for the large parallel values of κ, thus reducing the transfer of heat towards the drain; i.e., the number of participating modes decreases [20,21]. By using different physical parameters (temperatures, sizes, separation distances, etc.), several functions can be assigned to this system which can become either (i) a thermal switch, (ii) a thermal modulator, or (iii) a thermal amplifier. We discuss below those operating modes. To do so, we show in Fig. 3 a plot of the net heat flux received by each part of the system in a particular configuration where $\delta = 50$ nm, $d = 100$ nm, $T_S = 360$ K, and $T_D = 300$ K. The thickness of the gate and the separation distances have been chosen in order to avoid size effects and to keep the near-field heat flux sufficiently

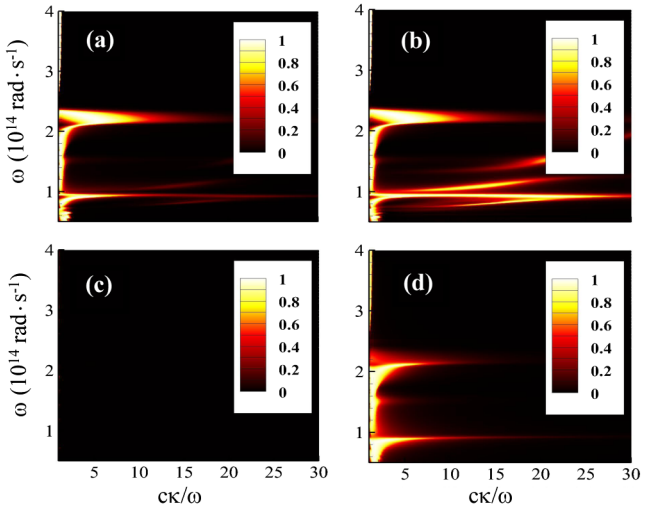

FIG. 2 (color online). Transmission probabilities of energy carried by the modes. Efficiency of coupling of modes (ω, $\boldsymbol{\kappa}$) in a SiO_2-VO_2-SiO_2 system ($\delta = 50$ nm and $d = 100$ nm). (a) $\mathcal{T}_p^{S/G}$ and (b) $\mathcal{T}_p^{G/D}$ with VO_2 in its crystalline state. (c) $\mathcal{T}_p^{S/G}$ and (d) $\mathcal{T}_p^{G/D}$ with VO_2 in its amorphous state. Wien's frequency (where the transfer is maximum) at $T = 340$ K is $\omega_{\mathrm{Wien}} \sim 1.3 \times 10^{14}$ rad/s. The dielectric permittivity of SiO_2 is taken from the database [19].

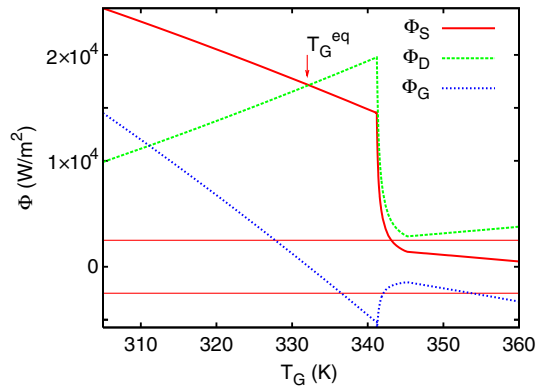

FIG. 3 (color online). Operating regimes of near-field thermal transistor. When T_G^{eq} is a little bit smaller than the critical temperature T_c of the IMT material, a small amount of heat applied on the gate induces a strong switching of heat fluxes Φ_D and Φ_S owing to its phase transition. By changing the flux Φ_G supplied to the gate, different functions (thermal switching, thermal modulation, and thermal amplification) can be performed. The fluxes plotted here correspond to a gate of VO_2 [8] with thickness $\delta = 50$ nm located at a distance $d = 100$ nm from two massive silica samples [19] maintained at $T_S = 360$ K and $T_D = 300$ K.

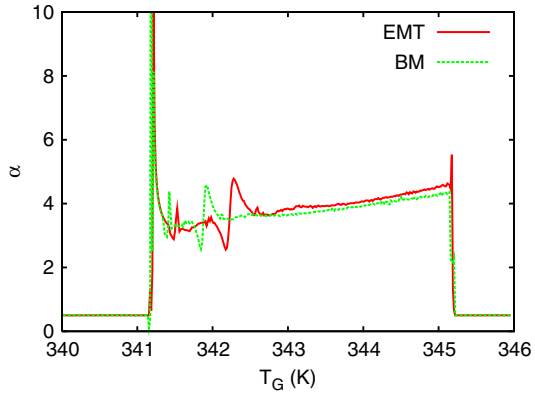

FIG. 4 (color online). Amplification factor α of the NFTT. When $T_G \ll T_c$ or $T_G \gg T_c$ the slopes of Φ_S and Φ_D are almost identical (modulo the sign) so that $\alpha \approx 1/2$. On the contrary, in the close neighborhood of T_c, we have $\alpha > 1$, owing to the negative differential thermal resistance in the transition region. Here, the parameters of the NFTT are the same as in Fig. 3. (EMT, effective medium theory; BM, Bruggeman mixing rule.).

large. Nevertheless, the presence of size effects could be taken into account without difficulty by using the appropriate optical properties.

Thermal switching.—In the situation depicted in Fig. (3), we have $T_G^{\mathrm{eq}} = 332$ K. An increase of T_G by about 10 deg (Φ_G is increased, in absolute value, by $\sim 10^{-8}$ W/μm^2) leads, as clearly shown in Fig. 3, to a reduction of heat flux received by the drain and lost by the source by more than 1 order of magnitude. That means our NFTT can be used in two operating modes where T_G is slightly below or above the critical temperature T_c, where in the case of $T_G < T_c$ we are in the "on" mode and for $T_G > T_c$ we are in the "off" mode.

Thermal modulation.—Over the temperature region around T_G^{eq} (strip between the vertical lines in Fig. 3), the heat current Φ_G over the gate remains quite small (i.e., $\Phi_S \sim \Phi_D$) while the flux received by the drain or lost by the source can be modulated from high to low values. The thermal inertia of the gate as well as its phase transition delay defines the time scale at which the modulator can operate. A much larger modulation of fluxes can be achieved with the NFTT when using $T_G^{\mathrm{eq}} \approx T_c$. Then the flux can be modulated over 1 order of magnitude by a small temperature change of T_G.

Thermal amplification.—The most important feature for a transistor is its ability to amplify the current or electron flux towards the drain. In the region of the phase transition around T_c, we see in Fig. 3 that an increase of T_G leads to a drastic reduction of flux received by the drain. This corresponds to a negative differential thermal conductance as recently described for SiC in Ref. [15] (note that this behavior does not violate the second principle of thermodynamics because the heat flux continues to flow from the hot to the cold body). Having a negative differential thermal conductance is the key for having an amplification, which is defined as (see, for example, Ref. [2])

$$\alpha \equiv \left| \frac{\partial \Phi_D}{\partial \Phi_G} \right| = \frac{1}{\left| 1 - \frac{\Phi_S'}{\Phi_D'} \right|}, \tag{6}$$

where

$$\Phi_{S/D}' \equiv \frac{\partial \Phi_{S/D}}{\partial T_G}. \tag{7}$$

It can be easily seen from Fig. 3 that $\alpha = 1/2$ for T_G much smaller or larger than T_c where the material properties of VO_2 are more or less independent of T_G, since $\Phi_S{}' = -\Phi_D{}'$. On the other hand, inside the transition region of VO_2, that means for temperatures around T_c the material properties of VO_2 change drastically, showing a negative differential thermal resistance or conductance, which leads to an amplification, i.e., $\alpha > 1$. This behavior is qualitatively demonstrated in Fig. 4, where the dielectric permittivity of VO_2 in the transition region is modeled using either a Bruggeman mixing rule as introduced in Ref. [7] or the classical effective medium theory. Hence, by choosing the temperatures such that $T_G^{\mathrm{eq}} \approx T_c$, the NFTT works as an amplifier.

The ability to control the flow of heat at the subwavelength scale in complex architectures of solids out of contact opens up new opportunities for an active thermal management of dissipating systems. It also suggests the possibility to develop contactless thermal analogs of electronic devices, such as thermal logic gates and thermal memories, for processing information by utilizing thermal photons rather than electrons. Unlike other schemes for creating thermal transistors, which thus far have been based on the control of acoustic phonons, the present concept authorizes much higher operational speeds (speed of light) and should be very competitive compared to the previous ones. We think also that the near-field thermal transistors could find broad applications in MEMS or NEMS technologies where they could be used, for instance, to generate mechanical works by modulating the heat flux received by the drain, by using microresonators such as cantilevers in contact with it. Finally, a far-field version of this transistor could also be considered but with much weaker flux exchanged between the basic elements because of the natural limit set by the Stefan-Boltzmann law.

The authors acknowledge financial support by the DAAD and Partenariat Hubert Curien Procope Program (Project No. 55923991)

*pba@institutoptique.fr
†s.age.biehs@uni-oldenburg.de

[1] J. Bardeen and W. H. Brattain, Phys. Rev. **74**, 230 (1948).

[2] B. Li, L. Wang, and G. Casati, Appl. Phys. Lett. **88**, 143501 (2006).
[3] L. Wang and B. Li, Phys. Rev. Lett. **99**, 177208 (2007).
[4] N. Li, J. Ren, L. Wang G. Zhang, P. Hänggi, and B. Li, Rev. Mod. Phys. **84**, 1045 (2012).
[5] E. Ozbay, Science **311**, 189, (2006).
[6] H. Caglayan, S.-H. Hong, B. Edwards, C. R. Kagan, and N. Engheta, Phys. Rev. Lett. **111**, 073904 (2013).
[7] M. M. Qazilbash, M. Brehm, B. G. Chae, P.-C. Ho, G. O. Andreev, B. J. Kim, S. J. Yun, A. V. Balatsky, M. B. Maple, F. Keilmann, H. T. Kim, and D. N. Basov, Science **318**, 1750 (2007).
[8] A. S. Barker, H. W. Verleur, and H. J. Guggenheim, Phys. Rev. Lett. **17**, 1286 (1966).
[9] P. J. van Zwol, K. Joulain, P. Ben-Abdallah, J. J. Greffet, and J. Chevrier, Phys. Rev. B **83**, 201404(R) (2011).
[10] P. J. van Zwol, K. Joulain, P. Ben-Abdallah, and J. Chevrier, Phys. Rev. B **84**, 161413(R) (2011).
[11] P. J. van Zwol, L. Ranno, and J. Chevrier, Phys. Rev. Lett. **108**, 234301 (2012).
[12] C. Starr, J. Appl. Phys. **7**, 15 (1936).
[13] N. A. Roberts and D. G. Walker, Int. J. Thermal Sci. **50**, 648 (2011).
[14] C. R. Otey, W. T. Lau, and S. Fan, Phys. Rev. Lett. **104**, 154301 (2010).
[15] L. Zhu, C. R. Otey, and S. Fan, Appl. Phys. Lett. **100**, 044104 (2012).
[16] E. Nefzaoui, J. Drevillon, Y. Ezzahri, and K. Joulain, arXiv:1306.6209v1.
[17] P. Ben-Abdallah and S.-A. Biehs, Appl. Phys. Lett. **103**, 191907 (2013).
[18] R. Messina, M. Antezza and P. Ben-Abdallah, Phys. Rev. Lett. **109**, 244302 (2012).
[19] *Handbook of Optical Constants of Solids*, edited by E. Palik (Academic, New York, 1998).
[20] S.-A. Biehs, E. Rousseau, and J.-J. Greffet, Phys. Rev. Lett. **105**, 234301 (2010).
[21] P. Ben-Abdallah and K. Joulain, Phys. Rev. B **82**, 121419(R) (2010).